

## Analysis of a “phase transition” from tumor growth to latency

P. P. Delsanto,<sup>1</sup> A. Romano,<sup>1</sup> M. Scalerandi,<sup>1</sup> and G. P. Pescarmona<sup>2</sup>

<sup>1</sup>*INFM, Dipartimento di Fisica, Politecnico di Torino, 10129 Torino, Italy*

<sup>2</sup>*Dipartimento di Biologia, Genetica e Chimica Medica, Università di Torino, Torino, Italy*

(Received 29 December 1999)

A mathematical model, based on the local interaction simulation approach, is developed in order to allow simulations of the spatiotemporal evolution of neoplasies. The model consists of a set of rules, which govern the interaction of cancerous cells among themselves and in competition with other cell populations for the acquisition of essential nutrients. As a result of small variations in the basic parameters, it leads to four different outcomes: indefinite growth, metastasis, latency, and complete regression. In the present contribution a detailed analysis of the dormant phase is carried on and the critical parameters for the transition to other phases are computed. Interesting chaotic behaviors can also be observed, with different attractors in the parameters space. Interest in the latency phase has been aroused by therapeutical strategies aiming to reduce a growing tumor to dormancy. The effect of such strategies may be simulated with our approach.

PACS number(s): 87.10.+e, 02.60.Cb

### I. INTRODUCTION

The most striking property of living systems is their adaptability to a changing environment. That means they are sensitive to local variations of many factors including temperature, oxygen tension, mechanical stress, nutrients concentration, hormones, and cytokines. Typically these quantities are not evenly distributed in space, leading to the formation of concentration gradients. Moreover, in a complex system local conditions are expected to change randomly with time.

One of the major tasks of living systems is feeding, since all of them are dissipative and require a continuous supply of O<sub>2</sub> and nutrients, both for performing work and reproducing. In the case of cell reproduction, all the cell structures must be duplicated and the need for each of the involved chemical components is absolute. These include glucose, aminoacids, metal ions (Fe<sup>2+</sup>, Zn<sup>2+</sup>, Cu<sup>2+</sup>, Na<sup>2+</sup>, K<sup>+</sup>), and phosphate. Any time the local concentration of some nutrient is scarce, living cells are compelled to move in the direction of the lacking nutrient [1] or to increase their affinity for it [2].

Since living systems grow esponentially until nutrients (or space) become a limiting factor and life on earth dates from at least  $3 \times 10^9$  yr, nutrient scarcity is the rule in almost any environment. Nutrient limitations lead to a competition among individuals: the ones with the highest capability for harvesting nutrients (e.g., cells with the largest receptors number or affinity) will be favored and survive. Usually affinity of a cell for a nutrient is inversely correlated to the nutrient concentration and the average uptake is kept constant through alternating oscillations of nutrient concentration and receptors number.

In a non-neoplastic cell population the balance between nutrients and receptors allows cell proliferation only to replace dead cells without a net increase of the cells number. By contrast cancer cells in the clinical stage of the disease display exponential growth. Reports in the literature show that in some cases cancer cells behave for a long time like normal cells (latency) and then suddenly start to grow expo-

entially, without any apparent major change in the host metabolism.

A realistic model of tumor growth, incorporating the mechanisms responsible for this kind of behavior, may be a valuable tool, not only for understanding the biodynamics involved, but also as a support for diagnosis and therapy. Hence numerous models of cancer growth [3,4] have been proposed in recent years. However, in the quest for an analytical solution, they have often been subject to overrestrictive or oversimplifying assumptions. As an alternative, computer simulation techniques may be used. Taking advantage of the rapidly increasing availability of high-performance supercomputer resources, they allow one to treat models of extreme complexity and nonlinearity.

We have recently proposed a model of cancer growth [5,6], based on the local interaction simulation approach (LISA) [7,8]. Our model aims at a prediction of the spatiotemporal evolution of neoplasies, conceived not as geometrical objects with assigned boundary conditions and internal properties, but rather as a grouping of identical, yet individual cells. The cancer growth is then the result of a set of rules, acting at the local level (i.e., applied to each cell individually), which govern the interactions of cancerous cells with other populations. They are by no means arbitrary, but they follow as a consequence of the competition for essential nutrients and other biological mechanisms suggested to us by what we learn from natural evolution at all levels. These “rules of the game” and their mathematical implementation are discussed in detail in Secs. II and III, respectively.

The purpose of a previous paper [5] was to illustrate the consistency of the proposed model and to prove that the corresponding system is extremely sensitive to small variations in the values of the relevant parameters. Our solutions confirmed that the process of cancer growth is strongly related to the environmental conditions and, in particular, to the availability of basic nutrients. Accordingly, it was proved that a manifold of different morphologies, growth rates, and outcomes (death, metastasis, and latency) can unfold. A variety of simulations results, mostly leading to indefinite tu-

mor growth, were also presented. The emergence of different outcomes as a result of small variations in the basic parameters is also demonstrated in Sec. IV of the present contribution. The main purpose here is, however, to analyze in detail the region in parameters space in which latency prevails. It is shown in Sec. V that the transition between the two regions of latency and indefinite growth is discontinuous and the critical parameters are computed. It is also proved (Sec. VI) that the transition may be induced by the action of a proper chemical, which acts on the nutrient supply. The results are in qualitative agreement with the experimental findings of Ref. [9].

## II. BIOPHYSICAL MODEL

The basic biophysical model at the two-dimensional (2D) level consists of a discretization of the slab of tissue considered in a rectangular grid [5]. At each gridpoint, the density of cancerous, necrotic, healthy, and other kinds of cells (which might be included in a more realistic treatment) and the various nutrients concentrations are defined. An initial tumoral seed is located in one or more gridpoints and allowed to evolve according to the following basic mechanisms.

(i) Feeding: the free nutrient  $p$ , which diffuses from one or more blood vessels into the tissue, is transformed into bound nutrient by both cancerous and healthy cells [10,11],  $p_0$  being the nutrient availability in the vessels. The amount of nutrient absorbed by cancer cells is proportional to the nutrient availability through a coefficient  $\gamma^{as}$ , as long as we are far from saturation.

(ii) Consumption: the bound nutrient is consumed by cancer cells at a rate  $\beta$  in order to sustain metabolic functions.

(iii) Cell death (apoptosis): cancer cells may die when the average amount of bound iron per cell ( $q$ ) falls below a given threshold  $Q_D$ .

(iv) Cell multiplication (mitosis): if  $q$  becomes larger than a given threshold  $Q_M > Q_D$ , cancer cells may reproduce.

(v) Diffusion: if the free nutrient available in the neighborhood is scarce, some cancerous cells may migrate with a diffusion rate  $\alpha$  to neighboring nodes, looking for “richer pastures” [12,13]. If the diffusion brings cancerous cells into a blood vessel, metastasis occurs [14].

TABLE I. List of the parameters used for the various cases.

$Q_M$	$Q_D$	$P$	$a$	$\beta^{as}$	$\Gamma$
0.8	0.2	1.0	0.2	0.005	0.1

As a result of these biological processes and their interplay, the system may evolve, according to the environmental conditions and, in particular, to the nutrient supply [15], towards four possible outcomes.

(i) Indefinite or explosive growth and eventual death of the patient.

(ii) Metastasis: the metastasized cells may land somewhere else and seed there a possibly more lethal tumor.

(iii) Latency (or dormancy): the volume of the neoplastic tissue remains almost constant for a very long time. Eventually, however, a small perturbation in the environmental conditions may lead to catastrophic growth [16]. A strong interest in the latency phase has been aroused by new therapeutical strategies, which have been recently developed in order to reduce a growing tumor to dormancy [17].

(iv) Complete regression (disappearance) of the tumor.

## III. MATHEMATICAL IMPLEMENTATION

The biophysical model, which has been discussed in the preceding section, requires a mathematical algorithm which allows one to treat individual cells (or groups of cells) individually and independently. The same is true for other ingredients of the model, such as the amount of (free or bound) nutrient. Therefore, any mathematical treatment which considers a tumor as a single entity in the shape, e.g., of an ellipsoid and endeavors to predict the time evolution of its geometry *a priori* excluded. By contrast, LISA, which allows one to treat independently local mechanisms of interaction among different individuals of the various populations (of cells, nutrients, etc.), seems to be the method of choice. As an additional advantage, LISA is particularly suitable for parallel processing and is extremely flexible. In fact, it allows us to start with a simple model, including only the most basic features, and then to gradually extend its complexity in a controlled fashion, to make it more and more realistic.

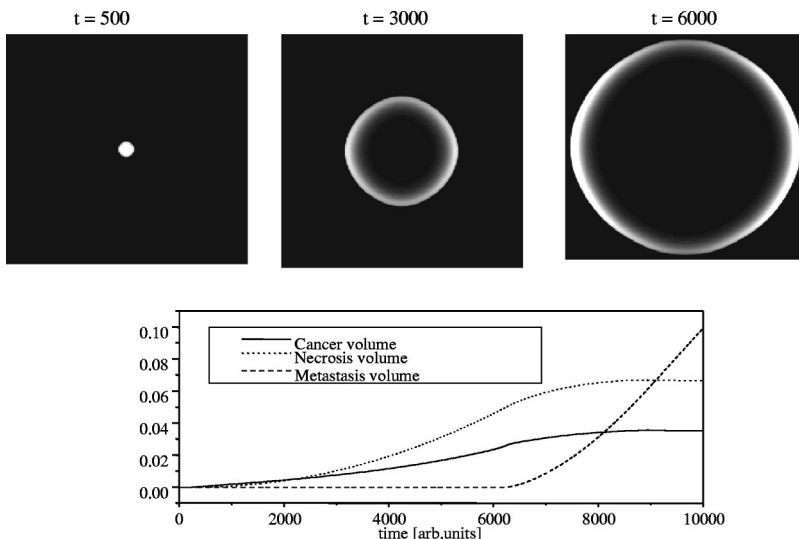


FIG. 1. Snapshots of the growing tumor at different times. Due to the high nutrient supply ( $p_0=0.2$ ), the final outcome is an indefinite growth of the neoplasia. All the “volumes” in the bottom plot are normalized to the initial volume of the tissue.

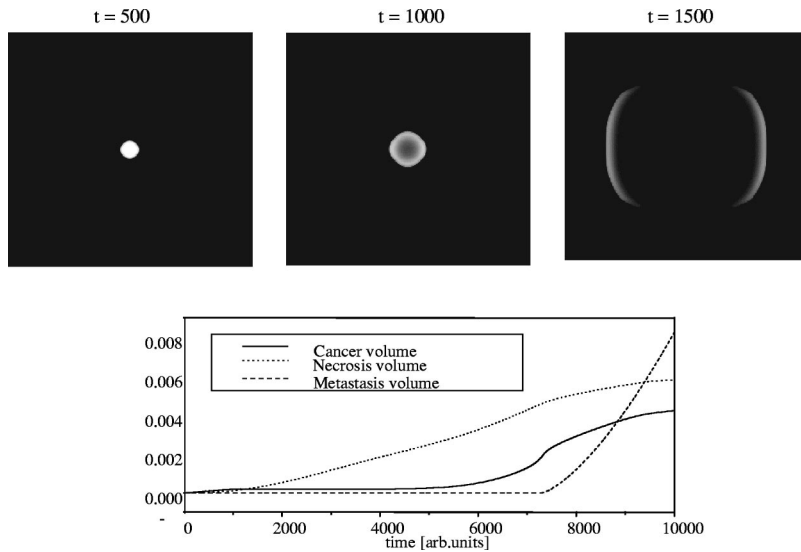


FIG. 2. Snapshots of the tumor for  $p_0=0.1$ . The final outcome is likely to be metastasis.

It may be instructive to compare LISA with a random walk procedure typical of a Monte Carlo approach. In a random walk simulation, one follows step by step the evolution of each particular cell, i.e., its nutrient consumption, random diffusion, mitosis, eventual apoptosis, etc. Since for each cell the next step is determined by the extraction of random numbers, the final outcome may be rather different for different simulations, even if the initial conditions and parameters are the same. By contrast, in a LISA simulation all processes which are allowed by the ‘‘rules of the game’’ occur simultaneously at each time step with an assigned rate. Thus LISA simulations may be viewed as providing an average over the outcomes of a large number of equally probable random walk experiments. Conversely LISA cannot supply microscopically detailed features, such as local fluctuations in the bulk or surface of the neoplasia.

In a LISA treatment, the ‘‘rules of the game,’’ which have been briefly discussed in the previous section, translate into a set of iteration equations for each space element or node (site) of the discretization grid. The complete set of iteration equations and their execution sequence have been described in detail in Ref. [5]. In the following, we limit ourselves to report only the most relevant equations, in order to provide at

least the ‘‘flavor’’ of the procedure.

If we consider for simplicity only one kind of nutrient (e.g., iron), the iteration equation for the number of cancerous cells  $c$  in any given site is given by

$$c^* = c[1 - r\Theta(cQ_D - q)] + r'\Theta(q - cQ_M), \quad (1)$$

where  $\Theta$  is the Heaviside’s step function and  $r$  and  $r'$  are random numbers between 0 and 1 (computed independently at each site and time). The local amount of bound nutrient  $q$  and the apoptosis and mitosis ‘‘per cell’’ thresholds,  $Q_D$  and  $Q_M$ , respectively, have already been defined in Sec. II. In Eq. (1) all the quantities refer to the time  $t$ , except  $c^*$ , which refers to the time  $t+1$  (time is also discretized). Equation (1) includes both rules (iii) and (iv) of Sec. II. In fact  $cQ_D - q > 0$  if the amount of bound nutrient per cell,  $q/c < Q_D$ , in which case apoptosis occurs with a random probability  $r$ . The same is true for mitosis.

Rules (i) and (ii) (nutrient feeding and consumption, respectively) yield the equations

$$\gamma = \gamma^{as}[1 - \exp(-\Gamma p)], \quad (2)$$

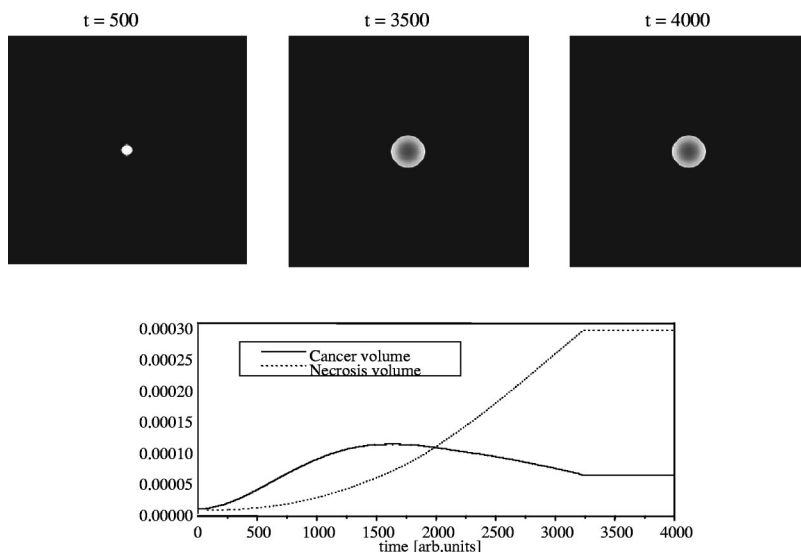


FIG. 3. Snapshots of the tumor for  $p_0 = 0.075$ . The final outcome is latency.

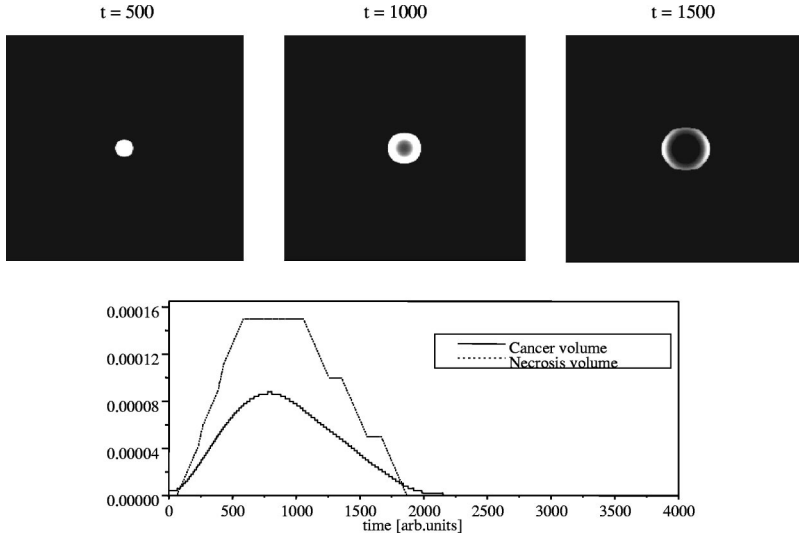


FIG. 4. Snapshots of the tumor for  $p_0=0.05$ . The final outcome is regression of the tumor (as can be inferred by the bottom plot).

and

$$\beta = \beta^{as} [1 - \exp(-q/c)], \quad (3)$$

where  $p$  is the free nutrient concentration at the site under consideration and  $\gamma^{as}$  and  $\beta^{as}$  represent asymptotic values. In fact, for small values of  $p$ , the feeding ratio  $\gamma$  increases linearly with  $p$ ; at higher concentrations, however, saturation occurs.  $\Gamma$  is a properly normalized iron affinity parameter. Similar considerations apply to the nutrient consumption.  $\gamma$  affects the amount of bound nutrient  $q$  and so enters the tumour dynamics, since it will affect the mitosis and apoptosis rates.

Finally, the diffusion of cancerous cells can be described by the equation

$$c^* = c + \sum_n \alpha_n c_n - 4\alpha c, \quad (4)$$

where  $n$  denotes the four neighboring sites and  $\alpha_n$  the diffusion rate of cancerous cells from them. Conversely  $4\alpha c$  represents the diffusion, assumed to be isotropic, from the site under consideration towards the four neighboring sites. Diffusion occurs only below a given threshold  $P$  of free nutrient per cell:

$$\alpha = a\Theta(cP - p), \quad (5)$$

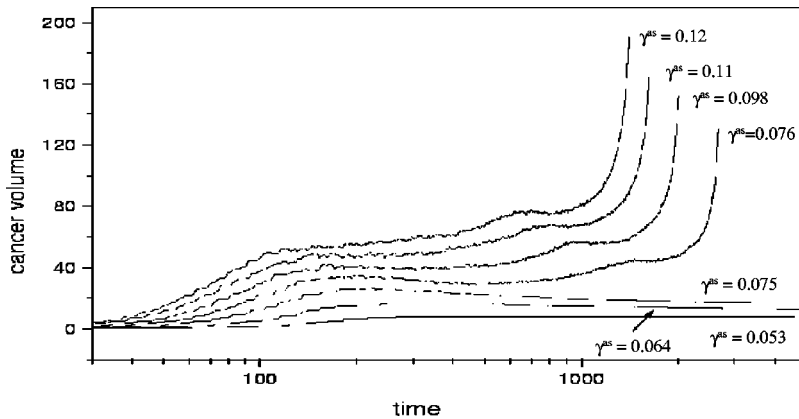


FIG. 5. Neoplastic growth evolution for different values of the nutrient affinity coefficient  $\gamma^{as}$  ( $p_0=0.03$ ).

where  $a$  is a coefficient depending on the time and space units considered.

Other equations can, of course, be added to include additional biodynamics mechanisms and make the treatment more realistic. The complexity of the model and the computational costs accordingly increase, but the approach remains basically the same.

#### IV. NEOPLASTIC GROWTH IN SOFT TISSUES

For our simulations we have considered a square specimen ( $300 \times 300$  gridpoints) with two blood vessels along the left and right edges of the tissue providing nutrient at a fixed rate  $p$ . The neoplasia is assumed to grow in a soft tissue and a single nutrient is considered. Generalizations to more nutrients and/or to tissues with anatomical barriers are currently in progress [18]. A small tumor seed is located in the center of the specimen at  $t=0$  and let evolve. The spatiotemporal evolution of the dynamic variables (number of cancer cells  $c$ , amount of free nutrient  $p$ , and bound nutrient  $q$  for each gridpoint of the tissue) can then be predicted for a large number of time steps. In all cases considered, the control parameters have been kept fixed, except for the nutrient availability in the vessels  $p_0$  and consumption  $\gamma^{as}$ . The values of the parameters are reported in Table I.

The spatiotemporal evolution of the system for different values of the nutrient supply is illustrated in Figs. 1–4 by means of snapshots of the concentrations of the tumoral cells

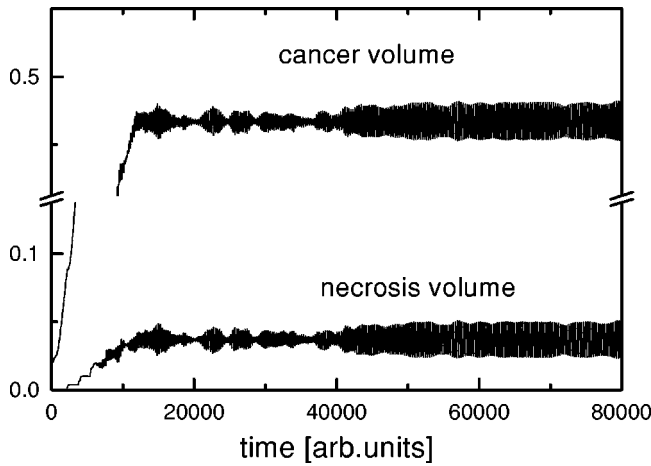


FIG. 6. Time evolution of the cancerous and necrotic cells for a subcritical value of  $p_0$  ( $p_0=0.05$ ) in the dormant state ( $\gamma^{as}=0.0008$ ).

at three representative times (in arbitrary units). In all the figures, higher-concentration regions are depicted with lighter tones; dark regions surrounded by active cells represent the formation of a necrotic core. Finally, the linear plots yield the time evolution of the average concentration of cancerous and dead cells and the total number of cancerous cells that have migrated into the blood vessel (eventually leading to metastasis).

In order to exemplify all the possible outcomes, in Figs. 1–4 we illustrate the four cases of indefinite growth, metastasis, latency, and regression in the case of  $\gamma^{as}=0.03$ . All the values of the parameters and variables are in arbitrary units. If we assume a constant nutrient concentration in the

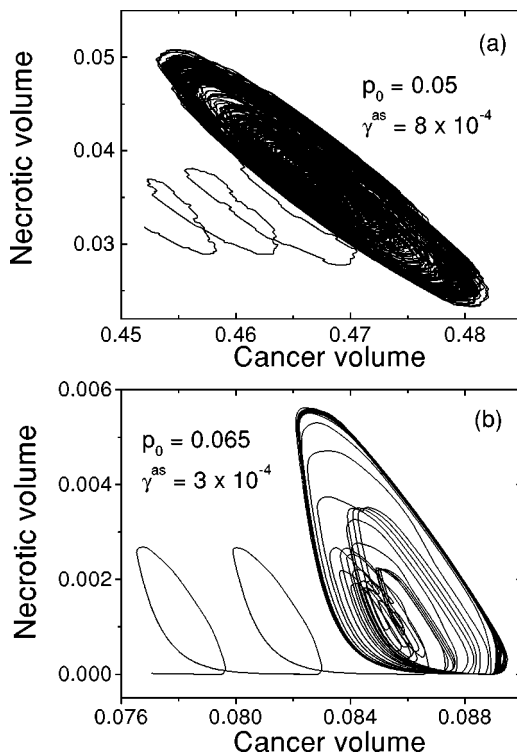


FIG. 7. Chaotic attractors in the phase space for two choices of values of the parameters  $p_0$  and  $\gamma^{as}$ .

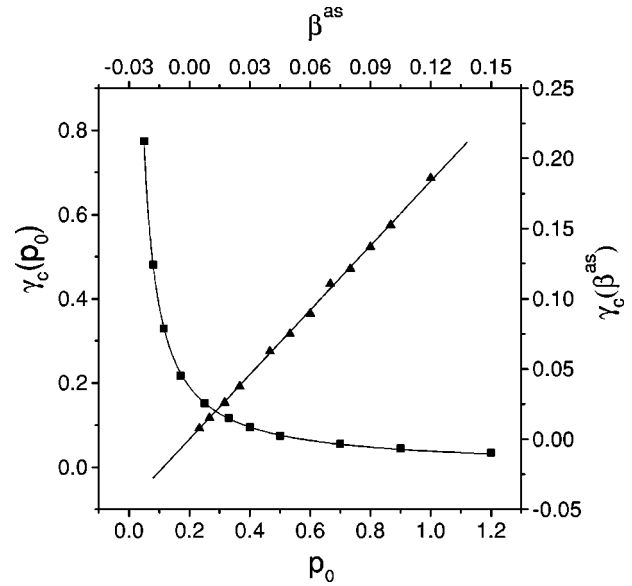


FIG. 8. Dependence of  $\gamma_c$  on the nutrient consumption rate  $\beta$  (triangles) and on the rate of available nutrient  $p_0$  (squares).

vessels  $p_0=0.2$ , the tumor grows very rapidly in all directions assuming a spheroidal shape (see Fig. 1). A large necrotic core is formed, surrounded by a ring of very active neoplastic cells. The likely outcome is death of the patient due to the tumor itself, before metastasis is likely to take place and possibly induce a new fatal tumor, as it can be inferred by the linear plots. Such a result is in agreement with clinical data regarding tumors developing in well vascularized soft tissues [19].

With a nutrient availability of  $p_0=0.1$ , cancer cells diffusion prevails against growth (see Fig. 2). In the initial stage of the evolution, the tumor assumes a spheroidal shape, like in the previous case. The number of active cells is, however, very small (note that the grayness scales are not the same in Figs. 1 and 2). At later times two active fronts are formed and propagate towards the vessels, leaving a small necrotic core behind. Even though the cells spread almost through the entire tissue, their total number is approximately constant up to  $t \sim 5000$  (see the linear plot) when the fronts get close to the vessel and find a large nutrient availability. There, cancerous cells proliferate quickly and growth predominates over diffusion. However, the tumor being close to the vessel, a large number of cells migrate into the vascular system (metastasis).

In Fig. 3 the nutrient supply is low ( $p_0=0.075$ ). The tumor grows spherically and soon reaches a stable configuration. Both cancer and necrotic volumes are practically stable, since apoptosis and mitosis take place at approximately the same rate. Meanwhile, macrophagi act in order to get rid of the newly formed necrotic cells. The outcome is therefore latency.

Finally, for an even lower nutrient availability ( $p_0=0.05$ ) regression of the neoplasia is observed (Fig. 4). The initial seed grows spherically. However, soon cancer cells start competing among themselves for the nutrient acquisition and cellular apoptosis prevails. Few cells are spread in a large area and they are rapidly reabsorbed. A necrotic core is also formed and very slowly reabsorbed by macrophagi. A

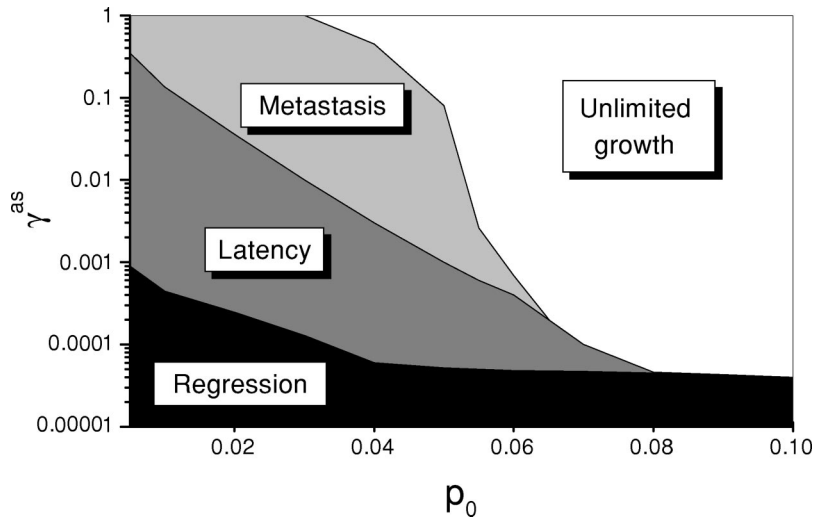


FIG. 9. Pictorial representation of the phase space in the nutrient availability–nutrient affinity space.

snapshot at a later time ( $t > 2500$ ) would show no more evidence of cancerous or necrotic tissue.

### V. PHASE TRANSITION TO TUMOR LATENCY

In order to analyze the phase transition from tumor growth to latency, in Fig. 5 we represent the total amount of cancer cells (volume in arbitrary units) vs  $t$  for different values of  $\gamma^{as}$  and a fixed value of  $p_0$  ( $p_0 = 0.03$ ). When the affinity for the nutrient is high,  $\gamma^{as} > \gamma_c$  ( $\gamma_c \approx 0.075$ ), the tumor grows indefinitely and metastasis is likely to occur. In a first phase ( $t < 100$ ) the growth is rather fast and spherical (snapshots are not shown here for brevity) in good agreement with clinical data [19]. At later times, after an almost quiescent state, the growth becomes explosive, leading to asymmetric shapes. A sharp ‘phase transition’ to latency occurs at  $\gamma^{as} = \gamma_c$ . In the region  $\gamma^{as} < \gamma_c$  the tumor grows up to a maximum size and then reaches a dormant (almost stable) configuration. For even smaller values of  $\gamma^{as}$  ( $\gamma^{as} < \gamma'_c \ll \gamma_c$ ), the available nutrient is not even able to support the original neoplastic seed and the tumor disappears altogether.

The behavior of the dormant stage depends strongly on the nutrient availability. For small values of  $p_0$ , the tumor reaches a completely stable state (see, e.g., the curve  $\gamma^{as} = 0.075$  in Fig. 5). Increasing the initial nutrient distribution, deterministic chaos appears, as shown in Fig. 6, with oscillations in the cancer and necrosis volumes of strongly variable amplitude. Such oscillations display a completely non-periodical behavior around a stable average value.

The ‘chaotic’ nature of the dormant stage for small values of  $p_0$  is further illustrated in Fig. 7 by means of plots in the cancer-volume–necrosis-volume space. Different chaotic attractors are formed, whose shape and properties depend on the value of both  $\gamma^{as}$  and  $p_0$ . The morphology of the tumor is, however, hardly affected. A similar behavior has been observed in other biological systems living in limiting nutrient concentrations [20], such as bacterial aggregations on a nutritional substrate [21].

Extensive numerical simulations have been used to calculate the critical value  $\gamma_c$  proving that it follows a simple scaling law (shown in Fig. 8) both with respect to the nutrient consumption rate  $\beta$  (to which it is proportional) and to the rate of available nutrient,  $p_0$  (to which it is inversely

proportional). The dependence on all other parameters is almost irrelevant. Figure 8 carries a very important consequence: when the nutrient concentration is high ( $p_0 > 0.4$ ), small changes of  $\gamma^{as}$  (of a size which is expected to happen randomly) can induce the transition between latency and indefinite proliferation, while changes in  $p_0$  are almost inconsequential. Conversely, for low values of  $p_0$  ( $p_0 < 0.2$ ), even very small changes in the nutrient concentration (induced, e.g., by proper therapies) can support the transition.

A complete representation of the behavior of the system in the parameter space is shown in Fig. 9. Here, we have assumed that metastasis occurs when the number of cells migrated into the vessel becomes larger than a given threshold  $\Xi$ , before the neoplastic volume becomes larger than a given volume  $\Lambda$ , assumed to be lethal for the patient. Both parameters  $\Xi$  and  $\Lambda$  are, of course, somewhat arbitrary and therefore the boundary between the two regions (metastasis and unlimited growth) is only representative. Several conclusions may be drawn from Fig. 9: e.g., regression may take place spontaneously for non-very-malignant tumors (i.e., those with low  $\gamma^{as}$ ) for whichever value of the nutrient supply. Unlimited growth is always a possible outcome, either for large  $\gamma^{as}$  or large  $p_0$ ; by contrast latency and metastasis are not expected if the nutrient supply is sufficiently large. We also observe that the chaotic region in the latency state,

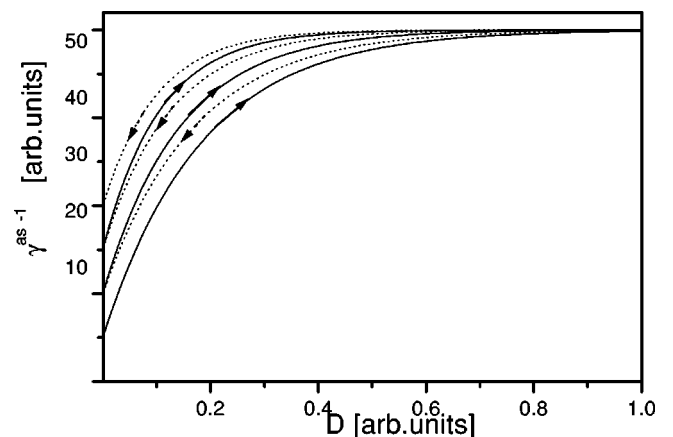


FIG. 10. Example of behavior of the hysteretic state equation between  $\gamma^{as}$  and the chemical concentration  $D$ .

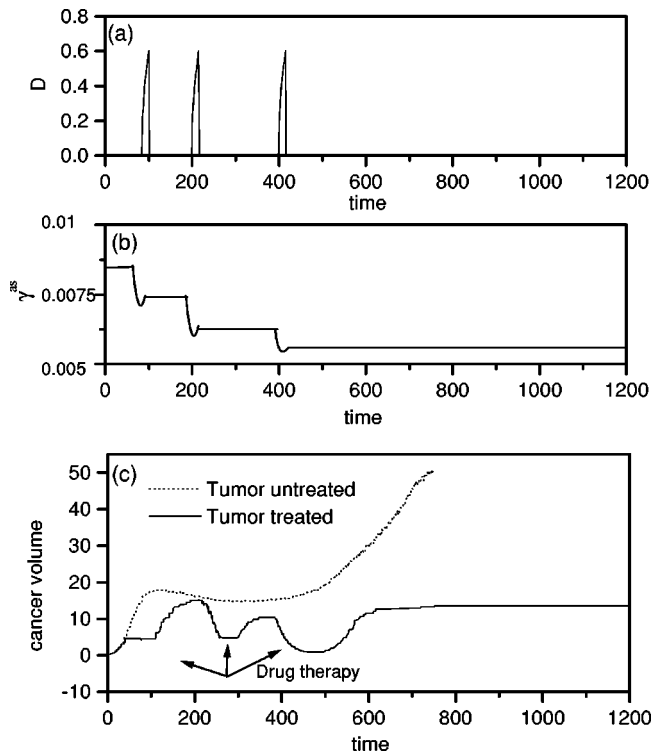


FIG. 11. Time evolution of (a) the drug concentration in the tissue during a three-cycle therapy protocol, (b) the corresponding value of  $\gamma^{as}$ , and (c) the consequent cancer growth profile (solid line). The dashed line refers to an untreated tumor with the same initial value of  $\gamma^{as}$ . All quantities are expressed in arbitrary units.

described in Figs. 6 and 7, corresponds to a region close to the triple point among regression, latency, and unlimited growth. Such a result is in agreement with general biological observations, which usually find that natural systems are close to instability and to a chaotic state.

## VI. THERAPY

The existence of a sharp transition between the dormant phase and the indefinite growth region, due to either small changes of  $p_0$  or  $\gamma^{as}$  according to the local conditions, has important implications for cancer therapy. In fact it is expected that the normal range of relevant parameters lies in a rather narrow band around critical values [22,23]. There a properly delivered therapeutical agent may induce the transition towards latency. To be more specific, let us assume that the effect of a certain drug is to inhibit the absorption of a given nutrient (e.g., antibodies against transferrin receptors [2]). Drug molecules diffuse to the target region and may attach to cancer cell receptors and occupy channels, which are normally used to acquire nutrients. In this process they act as decoys, thus reducing drastically the number of available receptors. In our model, this mechanism is equivalent to a sudden decrease of the parameter  $\gamma^{as}$ .

Usually the above process is reversible, since the decoys are quickly reabsorbed by the tissue. Then  $\gamma^{as}$  goes eventually back to its initial value and the effect of the therapy is reduced to just slowing down momentarily the tumor growth. The entire process can be easily simulated with LISA and snapshots of the tumor growth may be obtained at relevant

times (not shown here for brevity).

Other chemicals, however, act in a nonreversible way: e.g., they may change the receptors, so that they no longer fit and therefore do not absorb the nutrients. Or they may be metabolized and modified, so that they can bind to different receptors, again inhibiting nutrient absorption, i.e., effectively reducing the value of  $\gamma^{as}$ . Such a process may be introduced in our model by defining a hysteretic (multivalued) state equation between  $\gamma^{as}$  and the chemical concentration  $D$ . An example of the behavior of such a state equation is reported in Fig. 10.

Figure 11 simulates the effect of therapy by means of such an ‘‘irreversible’’ kind of drug. Figure 11(a) shows the drug concentration in the tissue, when a three-cycle protocol is applied. Figure 11(b) displays the effect on  $\gamma^{as}$  of the drug, for the  $\gamma^{as}$ - $D$  state equation reported in Fig. 10. One can observe three phases of alternatively decreasing and increasing values of  $\gamma^{as}$  in correspondence with the three peaks of drug concentration in Fig. 11(a), with a final value  $\gamma_F^{as}$  lower than the initial value  $\gamma_0^{as}$ . Correspondingly, Fig. 11(c) shows alternating phases of reduction and growth in the tumor size (continuous line). If  $\gamma_F^{as} < \gamma_c$ , at the end of the three-cycle therapy, latency is achieved even if  $\gamma_0^{as} > \gamma_c$ . By contrast, the dotted line, which refers to the case of an untreated tumor with the same initial value  $\gamma_0^{as}$ , shows indefinite growth.

Such a behavior is qualitatively similar to that recorded by Boehm *et al.* in experiments which aimed to test the effect of endostatin on different tumors in mice [9]. Endostatin is a chemical affecting the capability of endothelial cells to proliferate and consequently the occurrence of angiogenesis. In their experiments they have proved that a therapy protocol based on endostatin can induce latency after a suitable number of applications.

## VII. CONCLUSIONS

We have developed a mathematical model, based on the local interaction simulation approach, which aims to a simulation of the spatiotemporal evolution of neoplasies. The model consists of a set of ‘‘rules of the game,’’ which govern the interaction of cancerous cells among themselves and in competition with other cells populations for the acquisition of essential nutrients. Although at the present time the comparison between the results of our simulations and of clinical experiments may be only qualitative, we believe that the proposed approach may be useful for better understanding the basic biodynamics of cancer growth. In fact, one of the major drawbacks of current hypotheses about cancer growth is that they are not able to predict (with the exception of few cases of chemical cancerogenesis) whether, in the absence of clear-cut changes in the metabolic status of the host, cancer develops or not.

Our model shows that cancer cells in the dormant state (which is not different from the behavior of normal cells) display a ‘‘chaotic’’ nature, which is strictly dependent on the specific value of  $\gamma_c$ . A small increase (probably undetectable in living organisms) of  $\gamma_c$  leads to a state of exponential growth. If this behavior will be confirmed *in vivo*, it will be possible to explain the almost complete failure of primary prevention of cancer using biochemical parameters

and maybe suggest a different approach.

Our simulations can also be used if the proposed model of therapy as a forced and irreversible “phase transition” in parameter space is confirmed as a tool (a) for selecting the type of drug aimed to reduce either  $\gamma_c$  or  $p_0$ , according to the local conditions; (b) for optimizing the number of drug applications and/or the time interval between successive applications; (c) for deciding on the relative amounts of drug; (d) for predicting the latest useful time of inception. In fact, Fig. 11(c) clearly shows that drug therapy becomes ineffectual once the tumor growth has progressed beyond a certain threshold. However, it also shows that when the parameters of the tumor are in the “chaotic” region, very low doses of drug can be effective in preventing growth. This leaves hope for the future application of much less toxic therapies than the ones currently in use.

For a quantitative comparison with actual clinical data, it is of course necessary to refer to a specific tissue and tumor (either at the 2D level or, after a straightforward modification

of the algorithm, with a 3D treatment). Then all quantities, instead of being expressed in terms of arbitrary units, can be specified quantitatively and meaningful predictions can be attempted. Even so, the model, as it is, is probably too preliminary for a realistic comparison, but, as mentioned before, the approach is very flexible and new “ingredients” can be easily added. An effort in this direction is presently in progress in the case of tumors affecting the larynx [18]. In this case, in fact, several effects which are not included in our model (e.g., angiogenesis) are usually negligible.

#### ACKNOWLEDGMENTS

The authors wish to thank Professor C. Buzano and M. Rasetti (Dip. to di Fisica, Politecnico di Torino, Italy) and Professor C.A. Condat (FAMAF, Cordoba, Argentina) for useful discussions. This work was supported by the INFM Parallel Computing Initiative.

- 
- [1] M.F. Carlevaro, A. Albini, D. Ribatti, C. Gentili, R. Benelli, S. Cermelli, R. Cancedda, and F.D. Cancedda, *J. Cell Biol.* **136**, 1375 (1997).
  - [2] L. Bianchi, L. Tacchini, and G. Cairo, *Nucleic Acids Res.* **27**, 4223 (1999).
  - [3] J.A. Adam and N. Bellomo, *A Survey of Models for Tumor-Immune Dynamic Systems* (Birkhauser, Boston, 1997).
  - [4] I. Prigogine, R. Lefever, *Comp. Biochem. Physiol. B* **67**, 389 (1980).
  - [5] M. Scalerandi, A. Romano, G.P. Pescarmona, P.P. Delsanto, and C.A. Condat, *Phys. Rev. E* **59**, 2206 (1999).
  - [6] G.P. Pescarmona, M. Scalerandi, C.A. Condat, and P.P. Delsanto, in *Materials Science of the Cell*, edited by B. Mulder, C.F. Schmidt, and V. Vogel, MRS Symposia Proceedings (Materials Research Society, Pittsburgh, 1997), p. 217.
  - [7] P.P. Delsanto, R.B. Mignogna, M. Scalerandi, and R.S. Schechter, in *New Perspectives on Problems in Classical and Quantum Physics*, edited by P.P. Delsanto and A.W. Saenz (Gordon and Breach, New Delhi, 1998), Vol. 2, pp. 51–74.
  - [8] R.S. Schechter, H. H. Chaskelis, R.B. Mignogna, and P.P. Delsanto, *Science* **265**, 1188 (1994).
  - [9] T. Boehm, J. Folkman, T. Browder, M.S. O'Reilly, *Nature* (London) **390**, 404 (1997).
  - [10] R. Halvorsrud and G. Wagner, *Phys. Rev. E* **57**, 941 (1998).
  - [11] Th. Hofer, J.A. Sherratt, P.K. Maini, *Physica D* **85**, 425 (1995).
  - [12] J.C.M. Mombach and J.A. Glazier, *Phys. Rev. Lett.* **76**, 3032 (1996).
  - [13] F. Schweitzer, W. Ebeling, and B. Tilch, *Phys. Rev. Lett.* **80**, 5044 (1998).
  - [14] J. Murray, *Mathematical Biology*, Biomathematics Text (Springer-Verlag, Berlin, 1993).
  - [15] J.W. Uhr, R.H. Sheuermann, N.E. Street, and E.S. Vitetta, *Nat. Med. (N.Y.)* **3**, 505 (1997).
  - [16] G.P. Pescarmona, P.P. Delsanto, M. Scalerandi, and C.A. Condat, *Med. Hypotheses* **53**, 497 (1999).
  - [17] H.J. Mauceri *et al.*, *Nature* (London) (London) **394**, 287 (1998); P. Blenziger *et al.*, *Nature Biotech.* **17**, 343 (1999).
  - [18] B. Capogrosso, P.P. Delsanto, M. Scalerandi, and M. Maggiano, (unpublished).
  - [19] G. Helmlinger, F. Yuan, M. Dellian, and R.K. Jain, *Nat. Med. (N.Y.)* **2**, 271 (1997).
  - [20] J. Kovar, P.W. Naumann, B.C. Stewart, and J.D. Kemp, *Pathobiology* **63**, 65 (1995).
  - [21] G. Golding *et al.*, *Physica A* **260**, 510 (1998).
  - [22] D.C. Malins, N.L. Polissar, S. Schaefer, Y. Su, and M. Vinson, *Proc. Natl. Acad. Sci. USA* **95**, 7637 (1998).
  - [23] A.J. Einstein, H.-S. Wu, and J. Gil, *Phys. Rev. Lett.* **80**, 397 (1998).